J Solid State Electrochem (2006) 10: 230–235
DOI 10.1007/s10008-005-0671-9

ORIGINAL PAPER

Leonardo Salgado · Gabriel Trejo · Yunny Meas
Teresa Zayas

Cyclic voltammetry and electrochemical quartz crystal microbalance studies of a rhodized platinum electrode in sulfuric acid solution

Received: 31 August 2004 / Revised: 22 November 2004 / Accepted: 9 March 2005 / Published online: 17 August 2005
© Springer-Verlag 2005

Abstract The adsorption properties of a rhodized platinum electrode in sulfuric acid were studied through simultaneous cyclic voltammetry (CV) and electrochemical quartz crystal microbalance (EQCM) measurements. The processes occurring at the Rh surface during the potential scan between 0.04 and 1.3 V were analyzed in terms of the changes in mass and charge. The apparent molar masses of the species adsorbed on Rh in different potential regions were determined from the mass–charge correlation. The results obtained suggest that the desorption of hydrogen *UPD* initially occurs in conjunction with the incorporation of mass due to the adsorption of bisulfate/sulfate ions between 0.04 V and 0.12 V; the apparent molar mass (M_1) in this potential region is consistent with that of bisulfate ion, assuming that one sulfate species occupies the site originally occupied by five H atoms. Between 0.12 V and 0.20 V, the apparent molar mass, M_2, is less than M_1. This result may be associated with a structural rearrangement of the adsorbed sulfate species. The apparent molar mass, M_3, was determined in the potential region of 0.20–0.56 V; the value obtained for M_3 suggests that the adsorbed species are hydrated bisulfate ions ($HSO_4^- \cdot 4H_2O$). Additionally, it was found that Rh oxides formed at the surface between 0.56 V and 1.3 V could not be directly identified from the correlation between charge and mass.

Keywords Rhodium electrode · Adsorption · Anions · EQCM

L. Salgado (✉)
Área de Electroquímica, Depto de Química,
Universidad Autónoma Metropolitana Iztapalapa,
Apdo. Postal 55-534, México, 09340, México
E-mail: lsj@xanum.uam.mx
Tel.: +52-55-58044671
Fax: +52-55-58044666

G. Trejo · Y. Meas
Centro de Investigación y Desarrollo Tecnológico en
Electroquímica (CIDETEQ), Parque Tecnológico Sanfandila,
Pedro Escobedo A.P. 064, Querétaro, 76700, México

T. Zayas
Posgrado de Ciencias Ambientales, Instituto de Ciencias,
Benemérita, Universidad Autónoma de Puebla, 14 Sur# 6301 Col.
Jardines de San Manuel, Puebla, 72570, México

Introduction

Rhodium in pure or alloy form is of considerable importance in heterogeneous catalysis [1–4], yet little is known about the electrocatalytic properties of rhodium-based systems. This situation has motivated interest in the electrochemical properties of such systems.

The electrosorption properties of hydrogen and oxygen on Rh electrodes in aqueous media have been widely documented in the electrochemistry literature [5–18]. In recent decades, the study of the adsorption of anions, onto polycrystalline or monocrystalline substrates or onto surfaces modified with metallic adatoms, has been facilitated by the introduction of auxilliary techniques for use in electrochemical studies, such as in situ FTIR spectroscopy [19], infrared reflection absorption spectroscopy (IRAS) [20, 21], radioactive labeling [22–25], electrochemical impedance spectroscopy (EIS) [26], and electrochemical quartz crystal microbalance (EQCM) [27, 28].

Horanyi et al. studied the adsorption of anions onto Rh electrodes using cyclic voltammetry (CV) and the radiotracer method [22–25]. They showed that in acidic solutions, bisulfates (sulfates), halide ions added to the medium, or species formed by decomposition of perchlorate ions on the rhodium surface, are adsorbed in the potential region in which hydrogen desorption occurs. The adsorption of bisulfate/sulfate ions onto Rh(111) and polycrystalline Rh electrodes depends on the potential and on the characteristics of the substrate surface [22]. De Moraes and Nart [19] studied the adsorption of sulfates onto Rh (*hkl*) electrodes with low Miller indices using in situ FTIR reflection spectroscopy.

They found that the anions are adsorbed as SO_4^{-2} and that the orientation of the substrate surface influences the quantity of sulfate adsorbed.

Comparative studies examining the adsorption of HSO_4^- /SO_4^{-2} onto Pt(111) and Rh(111) electrodes have shown that sulfate/bisulfate anions are adsorbed at more positive potential values onto Pt(111) compared to Rh(111). This difference is considered to be related to the values of the potential of zero charge of each metal [21].

Based on CV, radiotracer, and EQCM results, Wasberg et al. [27] concluded that the mass increase during the desorption of hydrogen UPD from Rh is due to the adsorption of HSO_4^- /SO_4^{-2} anions. In the case of Pt electrodes in aqueous media, the mass-increase during the desorption of H_{ads} has been attributed to the adsorption of water molecules [29]. Uchida et al. [30, 31] have utilized a convenient method to identify species adsorbed on Au (111) and polycrystalline Au electrodes in electrolyte solutions of $HClO_4$ and H_2SO_4. Their method is based on the Faradaic correlation between the changes in mass and charge that are obtained in simultaneous EQCM and CV measurements:

$$\Delta m = \frac{\Delta QM}{nF} \tag{1}$$

where Δm is the mass change per unit area, ΔQ is the charge density, M is the molar mass, n is the number of electrons transferred, and F is the Faraday constant. Equation 1 predicts a linear relation between Δm and ΔQ with a slope equal to M/nF. Thus, the apparent molar mass of adsorbed substances can be determined from the slope of the plot of Δm versus ΔQ. Santos et al. [32] applied the approximation of Uchida et al. [30, 31] to the interface between Pt and electrolytes ($HClO_4$, H_2SO_4, H_3PO_4 and HCl). Their results indicated that the desorption of H_{ads} occurs in conjunction with the adsorption of water molecules, and, in the double layer potential region, produces the adsorption of hydrated anions on the electrode surface. Recently, Oliveira et al. [28] used CV and EQCM to study the electrodeposition of Rh onto Pt in a perchloric acid solution. They identified the surface oxides of rhodium, produced during the potential scan, from the correlation between charge and mass.

In the present work, we studied the adsorption processes at the Rh–H_2SO_4 interface by means of simultaneous CV and EQCM measurements. These measurements allowed us to examine the correlation between mass change and charge with the aim of identifying the species adsorbed onto the Rh electrode surface as a function of potential.

Experimental

A 5-MHz AT-cut quartz crystal with a Pt film (Maxtek, Torrance, CA, USA) was used to prepare the rhodium electrode. The Pt–EQCM electrode in 1 M H_2SO_4 was cycled between 0.05 V and 1.50 V in order to clean the surface and obtain a reproducible *i–E* profile. Subsequently, the deposition of rhodium on the Pt–EQCM electrode was carried out by electrolysis at a controlled potential (0.15 V for 600 s) in a rhodium solution (2 g l^{-1}) that was prepared from $Rh_2(SO_4)_3{\cdot}4H_2O$ (*Alfa Easar* 99.99%) and concentrated sulfuric acid (Merck AR) [33]. The mass of Rh deposited onto the Pt–EQCM electrode was on the order of 27 μg.

The Rh–Pt–EQCM electrode was removed from the solution and rinsed with deionized water, after that it was introduced into 1 M H_2SO_4 and subjected to continuous potential cycles in the interval between 0.04 V and 1.3 V. The *i–E* profile obtained after ten cycles was consistent with that of a polycrystalline Rh electrode in 1 M H_2SO_4 [6, 7]. The real area of the rhodized electrode was determined from the charge of hydrogen desorption, Q_H, and the charge of 221 μC cm^{-2} associated with the charge of a monolayer of H adsorbed onto polycrystalline Rh [6]. The value obtained for the real area was 54 cm^2 and the roughness factor, f_r, was 39.5.

The electrogravimetric study of the rhodized platinum electrode in sulfuric acid solution was carried out in a conventional three-electrode cell with a water jacket. An electrochemical quartz crystal microbalance (EQCM; Maxtek, PM 710) and a PARC EG&G potentiostat galvanostat (model 263 A) controlled by independent computers running the software PM710 and M270, respectively, were used to measure the current and resonance frequency of the quartz crystal simultaneously. The EQCM signal was recorded as Δf ($=f-f_o$) against the electrode potential.

Thick films of even metals on quartz crystal may be subjected to nonlinear frequency responses as a consequence of impedance mismatch [34]. However, additional experiments of Faradaic deposition of Cu onto the Rh–Pt–EQCM electrodes showed a linear relationship in accordance with the Sauerbray equation [35]:

$$\Delta f = \frac{-2f_0^2\pi}{(\mu_q\rho_q)^{1/2}}\Delta m = -C_f\Delta m \tag{2}$$

where Δf (Hz) is the frequency change; Δm (ng cm^{-2}) is the mass change per unit area, μ_q is the shear modulus, ρ_q is the density of quartz, f_0 is the fundamental frequency of the resonator, and C_f (Hz ng^{-1} cm^2) is the sensitivity factor of the quartz crystal used in the measurements. The value of C_f was determined in independent experiments on the Faradaic deposition of Ag onto the Pt–EQCM electrode (0.053 Hz ng^{-1} cm^2).

A spectroscopic-grade graphite rod (PARC) was used as counter electrode and the reference was an Hg/Hg_2SO_4/K_2SO_4 saturated connected to the cell by means of a Luggin capillary. In this work, all potentials are referenced to the normal hydrogen electrode (NHE).

All experiments were performed in 1 M H_2SO_4, prepared from concentrated sulfuric acid (Merck AR), and ultrapure water (18 M cm). Prior to each experiment,

the solutions were deaerated with a flow of high-purity nitrogen. All experiments were carried out in an inert atmosphere (N_2) at room temperature (24 ± 1 °C).

Results and discussions

Figure 1 shows the voltammograms (Fig. 1a) and the corresponding mass changes (Fig. 1b) for the Rh–Pt–EQCM electrode in 1 M H_2SO_4 recorded at 20 mV s^{-1}. The upper potential limit, E_U, was modified from 0.5 V to 1.3 V in increments of 0.1 V in each cycle. In the positive potential scan, the voltammograms in Fig. 1a show three characteristic potential regions: region A (≤0.3 V), corresponding to the desorption of hydrogen UPD; region B (0.3–0.5 V), associated with the double layer charge and region C (0.5–1.3 V) corresponding to the formation of surface oxides. In the potential scan, in the negative direction, the reduction of surface oxides gives rise to the cathodic peak O_c, whose intensity and potential depend on E_U. As E_U is made more positive, peak O_c increases in intensity and is displaced to less positive potentials due to the greater amount and higher stability of the surface oxides formed; consequently, the interference between the reduction of surface oxides and the electroadsorption of H is more significant. The characteristics of the *j–E* profiles of the voltammograms in Fig. 1a are consistent with those reported previously for the same system [6, 7].

It is important to indicate that the film of Rh on the Pt–EQCM was stable in the potential interval applied in the experiments (0.04–1.3 V). In contrast, Joudkazis et al. [36] have reported an EQCM study of the anodic dissolution of Rh films in sulfuric acid. The results of their experiments, in which the deposition of Rh was performed on a Au–EQCM electrode, indicated that the anodic dissolution of the Rh film may be related to the weak adherence of the rhodium to the substrate.

The Δ*m–E* curves (Fig. 1b) show the mass changes at the Rh–Pt–EQCM electrode corresponding to the voltammograms in Fig. 1a ($0.9 \le E_U \le 1.3$ V). During the positive potential scan from 0.04 V to 1.3 V, four regions with distinct linear variations are observed in the Δ*m–E* plot. The corresponding mass changes (Δ*m*) are $\Delta m_I = 7.0$ ng cm^{-2}, located in region A between 0.04 V and 0.15 V; $\Delta m_{II} = 7.5$ ng cm^{-2}, which spans from region A to C (0.15–0.65 V); and $\Delta m_{III} = 8.7$ ng cm^{-2} (0.65–1.0 V) and $\Delta m_{IV} = 11.1$ ng cm^{-2} (1.0–1.3 V), which occur at potentials more positive than 0.65 V (region C). In addition, the Δ*m–E* curves (Fig. 1b) show that the hysteresis between the formation and reduction of surface oxides becomes more pronounced as the upper potential limit is increased.

Figure 2 shows in greater detail the voltammogram (curve a) and the corresponding mass change (curve b) of the Rh–Pt–EQCM electrode in the hydrogen region. From these plots, it is clearly seen that the adsorption and desorption of hydrogen involves a decrease and increase in mass, respectively. Results similar to the present Δ*m–E* data (Fig. 2) were previously reported by Wasberg et al. [27]. On the basis of the harmony of EQCM and radiotracer sorption results, obtained in the course of voltammetric study of a rhodized electrode, concluded that the mass increase during the desorption of hydrogen from rhodized electrodes is due to the adsorption of HSO_4^- (SO_4^{-2}) onto the Rh sites vacated by hydrogen.

The increase in mass on Pt electrodes in aqueous media during the desorption of hydrogen UPD has been discussed by Gloaguen et al. [29], who suggested that this mass increase is produced by the substitution of H with water molecules according to the following reaction scheme:

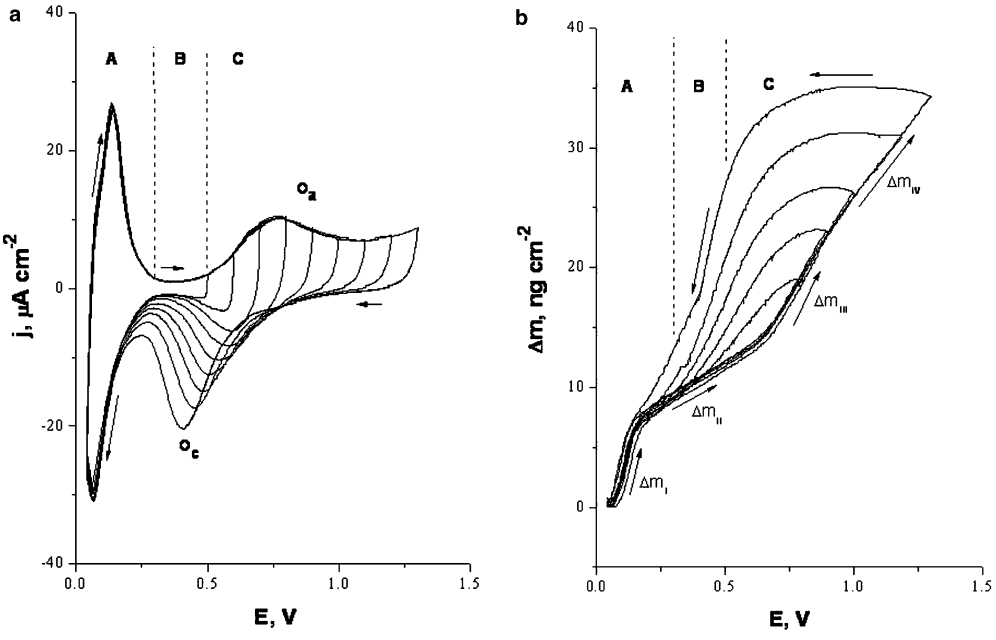

Fig. 1 **a** Voltammograms (*j–E*) for a Rh–Pt–EQCM electrode in 1 M H_2SO_4, $v = 20$ mV s^{-1}, with variation in the upper potential limit from 0.5 V to 1.3 V in increments of 100 mV and **b** the corresponding mass changes (Δ*m–E*) ($0.9 \le E_U \le 1.3$ V)

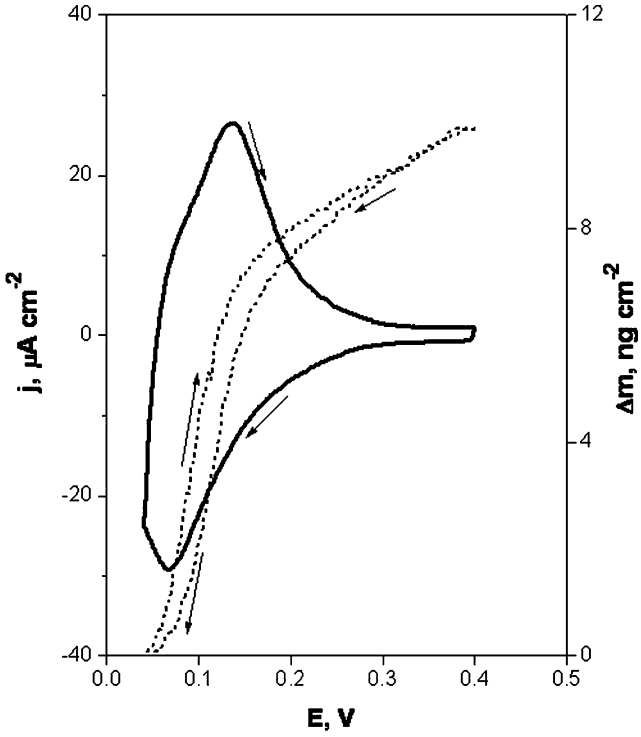

Fig. 2 **a** Voltammogram and **b** the corresponding mass changes (Δm–E) for a Rh–Pt–EQCM electrode in 1 M H_2SO_4 in the region of H UPD, $v = 20$ mV s^{-1}

$$Pt(H) + xH_2O \rightarrow Pt(H_2O)_x + H^+ + e^- \quad (3)$$

In support of this hypothesis, Santos et al. [32] have demonstrated the adsorption of water molecules on Pt by analyzing the correlation between mass and charge.

On the other hand, the mass variation Δm_{II} in the Δm–E curve (Fig. 1b) predominantly occurs in potential region B (the double layer region), and only partially in potential regions A and C. Various authors have attributed the mass increase in the double layer region to the adsorption of anions and water molecules [27, 28, 30–32].

In the potential region in which surface oxides are formed (region C, 0.5–1.3 V, Fig. 1b), the mass increases monotonically with increasing E_U. In this case, two important mass changes are observed: Δm_{III} between 0.65 V and 0.9 V and Δm_{IV} between 0.9 V and 1.4 V (Fig. 1b). This suggests the formation of two types of Rh-oxygen species in this potential region (0.65–1.3 V), which is consistent with the scheme for the formation of Rh surface oxides between 0.55 V and 1.40 V proposed by Peuckert [37] and Jerkiewicz et al. [18]:

$$Rh + H_2O \rightarrow RhOH + H^+ + e^- \quad 0.55 - 0.95\,V \quad (4)$$

$$Rh(OH) + 2H_2O \rightarrow Rh(OH)_3 + 2H^+ + 2e^- \quad 0.95 - 1.40\,V \quad (5)$$

From the voltammograms in Fig. 1a, the oxidation charge densities were obtained and corrected to account for the double layer charge. In the potential region of 0.5–1.0 V, the oxidation charge was 212 μC cm^{-2}, which is comparable with the charge of desorption of a monolayer of H_{ads} from polycrystalline Rh (221 μC cm^{-2}) [6]. This suggests that the formation of the surface oxide between 0.5 V and 1.0 V involves the transfer of one electron, consistent with reaction 4 for the formation of Rh(OH). However, in the potential interval of 1.0–1.3 V, the charge density was 123 μC cm^{-2}, which is far smaller than the value of 221 μC cm^{-2} for the desorption of a monolayer of H_{ads} from polycrystalline Rh; hence, the results are not consistent with the formation of $Rh(OH)_3$ via reaction 5.

The apparent molar mass of species adsorbed onto the Rh electrode surface during the positive potential scan (anodic half-cycle) was determined using Eq. 6, in agreement with the method proposed by Uchida et al. [30, 31]

$$\frac{M}{n} = \frac{\Delta m F}{\Delta Q} \quad (6)$$

The parameters in Eq. 6 are the same as those defined above for Eq. 1.

A plot of the variation in mass per unit area (obtained by EQCM) as a function of the charge density (determined by CV) (Δm versus ΔQ; Fig. 3) shows four linear variations in different potential regions, which may be associated with four types of species adsorbed on the Rh.

Based on Eq. 6, the slope ($d\Delta m/d\Delta Q$) in each of the four regions was multiplied by Faraday's constant, giving four apparent molar masses: $M_1/n = 18.7$ g mol^{-1} (0–0.12 V), $M_2/n = 3.8$ g mol^{-1} (0.12–0.20 V), $M_3/n = 174$ g mol^{-1} (0.20–0.56 V) and $M_4/n = 11$ g mol^{-1} (0.56–1.30 V).

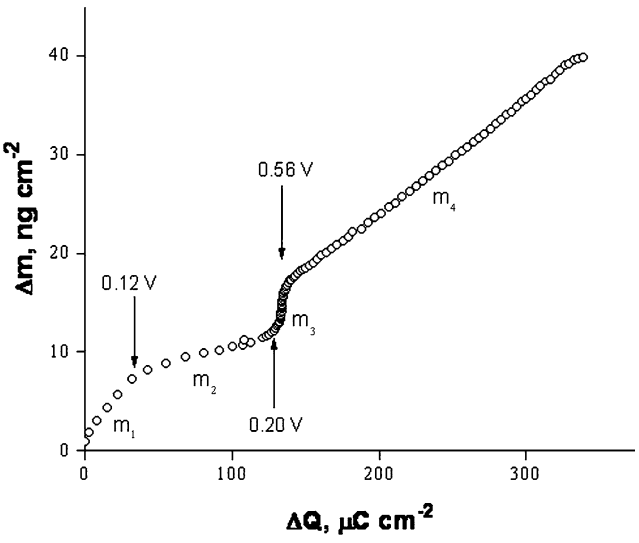

Fig. 3 Relation between the mass change per unit area, Δm, and the electric charge density, ΔQ, for the Rh–Pt–EQCM electrode in 1 M H_2SO_4 obtained from the data in the voltammograms and Δm–E curves in Fig. 1a and b, respectively

The molar masses M_1/n and M_2/n are associated with species adsorbed onto Rh in potential region A ($E \leq 0.3$ V), that is, during the desorption of hydrogen UPD. At first glance, the value of $M_1/n = 18.7$ g mol^{-1} suggests that water molecules are adsorbed onto the electrode during the desorption of hydrogen between 0.04 V and 0.12 V, as has been discussed by Gloaguen et al. for the case of Pt electrodes [29]. In addition, the molar mass $M_2/n = 3.8$ g mol^{-1} (0.12–0.20 V) suggests that a species of molar mass lower than M_1/n is involved in this potential region. However, a radiotracer study of the Rh–H_2SO_4 system by Wasberg et al. [27] showed that the H desorption from rhodized electrodes in sulfuric acid occurs simultaneously with the adsorption of sulfate ions HSO_4^- /SO_4^{-2} . This implies that the adsorption of one sulfate ion (HSO_4^- /SO_4^{-2}) onto Rh displaces a certain number of H adatoms (N_H), and thus that the sulfate ion occupies a certain number of active sites on the Rh surface (N_{RH}). Assuming that the H:Rh stochiometry of adsorption is 1:1 [6], then $N_H = N_{RH}$. When it is considered that the desorption of H from Rh is accompanied by the simultaneous adsorption of HSO_4^- /SO_4^{-2}, the apparent molar mass should be 97 g mol^{-1}, the value for a bisulfate ion. However, if it is assumed that one bisulfate/sulfate ion takes the place of five atoms of H_{ads} on Rh, then the resulting value of the apparent molar mass will be 97 g mol^{-1}/5, which equals 19.4 g mol^{-1}, close to the value of 18.7 g mol^{-1} obtained experimentally. Thus, we suggest that between 0.04 V and 0.12 V, the initial adsorption of each bisulfate/sulfate on Rh occupies five active sites previously occupied by H_{ads}.

In considering the validity of the above result, it is also necessary to account for the fact that on the basis of the cross sectional area of sulfate ion (0.183 nm^2) and the charge associated with the desorption of a H monolayer ($Q_{H,s} = 221$ μC cm^{-2}), the relation obtained between the number of sulfate ions adsorbed per square centimeter (54.6×10^{13} cm^{-2}) [22] and the number of H adatoms (1.38×10^{15} cm^{-2}) indicates that the number of H atoms displaced by one sulfate ion is 2.5. If this were correct, the value of $M_1/2.5$ would be expected to be 38.8 g mol^{-1}; however, the value obtained experimentally is 18.7 g mol^{-1}. Given that the experimental value is very different from 38.8 g mol^{-1} but close to 19.4 g mol^{-1}, it is reasonable to conclude that adsorption of a sulfate ion onto a polycrystalline Rh surface displaces five atoms of H_{ads}.

Between 0.12 V and 0.2 V, the value of M_2/n is 3.8 g mol^{-1}, which is much less than M_1/n. In this potential region (region A), it is reasonable to expect a value of the apparent molar mass similar to that of M_1/n for the adsorption of sulfate ions. However, the much lower value of M_2/n between 0.12 V and 0.20 V implies a change in the slope of the plot of Δm versus ΔQ (Fig. 3), with an important decrease in the mass per unit charge. One explanation for this result would be that it derives from a rearrangement of the sulfate ions adsorbed on the electrode surface, which could cause a decrease in the relation ($\Delta m/\Delta Q$) and consequently in the apparent molar mass. Thus, it is possible that in the potential region between 0.12 V and 0.20 V, a transition occurs from one spatial configuration of sulfate ions adsorbed to another, giving rise to a mass–charge relation that is not representative of the adsorbed species. Further experiments will be necessary to investigate the changes in apparent molar mass in this potential region.

The molar mass $M_3 = 174$ g mol^{-1} corresponds to the species adsorbed onto Rh between 0.20 V and 0.56 V (i.e., from region A through to the beginning of region C). Based on the value obtained for M_3/n, we propose that the species adsorbed in this potential region is the hydrated bisulfate ion, HSO_4^- ·4H_2O (168.06 g mol^{-1}). In a study of Pt in 0.1 M H_2SO_4, Santos et al. [32] determined a molar mass of 135 g mol^{-1} for the species adsorbed in the region of the double layer charge, which they assigned to the dihydrated bisulfate ion, HSO_4^-·2H_2O (133 g mol^{-1}). For Au in 0.1 M H_2SO_4, Uchida et al. [31] reported a molar mass of $M/n = 169$ g mol^{-1} corresponding to HSO_4^-·4H_2O. Uchida et al. [31] and Santos et al. [32] have indicated that the hydration value determined by EQCM may differ from the coordination of the anion in solution phase because the adsorbed anion may expell or accept hydration molecules in order to optimize its arrangement on the electrode surface.

In region C, the relation between mass and charge density exhibits a single slope ($d\Delta m/d\Delta Q) = m_4$, suggesting the presence of only one type of surface oxide. This behavior stands in contrast to the two in mass increases (Δm_{III} and Δm_{IV}) observed in the Δm–E curve (region C in Fig. 1b), suggesting the formation of two Rh-oxygen species. The calculated value of $M_4 = 11$ g mol^{-1} is less than the expected value of 17 g mol^{-1} for Rh(OH) [18, 37]; this discrepancy may be related to the desorption of hydrated anions during the formation of the surface oxide, as mentioned by Oliveira et al. [28] in relation to thin films of Rh in perchloric acid. Consequently, analysis of the correlation between mass and charge was not a satisfactory method for identifying the surface oxides of Rh.

The results obtained for the Rh–H_2SO_4 (1 M) system using EQCM and CV provide useful information on the adsorption phenomena that occur at the same time as the electrosorption of H and in the double layer region. However, analysis of the correlation between charge and mass proved to be an inappropriate method for determining the Rh oxides formed at the surface. Hence, it is necessary to devise future studies aimed at clarifying the deviations of the values of the apparent molar mass from the expected values in certain potential regions.

Conclusions

Rhodized Pt–EQCM electrodes were found to be appropriate for the study of the Rh–H_2SO_4 interface through simultaneous CV and EQCM measurements

due to the stability of the Rh film under the experimental working conditions. The quantitative correlation between the mass change per unit area and charge density can, in accord with the method proposed by Uchida et al. [30, 31], be used to determine the apparent molar masses of the species adsorbed onto Rh in the potential regions of hydrogen ($0.04 \leq E \leq 0.12$ V) and of the electric double layer (0.2 V$\leq E \leq 0.5$ V). The results obtained suggest that the desorption of hydrogen UPD initially ($E \leq 0.12$ V) occurs in conjunction with the adsorption of bisulfate/sulfate ions and, that one bisulfate/sulfate ion takes the place of five atoms of H_{ads} on Rh. The adsorption of hydrated anions ($HSO_4^- \cdot 4H_2O$) predominates from 0.20 V up to 0.56 V, where surface oxides begin to form. However, the surface oxides of Rh formed at the surface could not be determined directly from the correlation between mass and charge.

Acknowledgements We would like to thank CONACYT for financial support in the development of this study.

References

1. Griffith WP (2003) Platinum Metals Rev 47:175
2. Matolin V (1995) Fizika A 4:181
3. Snyder G, Tadd A, Abraham MA (2001) Ind Eng Chem Res 40:5317
4. Hess R, Krumeich F, Mallat T, Baiker A (2004) J Mol Catal A Chem 212:205
5. Woods R (1977) In: Bard AJ (ed) Electroanalytical chemistry, vol 9. Marcel Dekker, New York, pp 1–162
6. Rand DAJ, Woods R (1971) J Electroanal Chem 31:29
7. Pallota C, De Tacconi NR, Arvía AJ (1981) Electrochim Acta 26:261
8. Pallota C, De Tacconi NR, Arvía AJ (1983) J Electroanal Chem 159:201
9. Chialvo AC, Triaca WE, Arvía AJ (1987) J Electroanal Chem 237:237
10. Custidiano E, Piovano S, Arvía AJ, Chialvo AC, Ipohorski M (1987) J Electrtoanal Chem 221:229
11. Hourani M, Wieckowski A (1987) J Electroanal Chem 227:259
12. Wasberg M, Horanyi M, Wieckowski A (1990) J Electroanal Chem 278:425
13. Dunja C, Marijan V (1990) J Electroanal Chem 279:273
14. Florit MI, Bolzán AE, Arvia AJ (1995) J Electroanal Chem 394:253
15. Hiroyuki T, Akira S, Ken-Ichi T (1995) J Electroanal Chem 381:95
16. Wan L-J , Yau S-L, Swain GM, Itaya K (1995) J Electroanal Chem 381:105
17. Jerkiewicz G, Borodzinski JJ (1993) Lagmuir 9:2202
18. Gregory J, Alireza Z (1996) J Phys Chem 100:8454
19. De Moraes Ines R, Nart Francisco C (2001) J Braz Chem Soc 12:138
20. Shingaya Y, Ito M (1994) J Electroanal Chem 372:283
21. Shingaya Y, Ito M (1999) J Electroanal Chem 467:299
22. Zelenay P, Horanyi G, Rhee CK, Wieckowski A (1991) J Electroanal Chem 300:499
23. Wasberg M, Horanyi G (1995) J Electroanal Chem 385:63
24. Wasberg M, Horanyi G (1995) J Electroanal Chem 386:213
25. Horanyi G, Wasberg M (1996) J Electroanal Chem 404:291
26. Horvat-Radosevic V, Kvastek K (2004) J Electroanal Chem 566:451
27. Wasberg M, Bacskai J, Inzelt G, Horanyi G (1996) J Electroanal Chem 418:195
28. Oliveira RTS, Santos MC, Bulhoes LOS, Pereira EC (2004) J Electroanal Chem 569:233
29. Gloaguen F, Leger JM, Lamy C (1999) J Electroanal Chem 467:186
30. Uchida H, Ikeda N, Watanabe M (1997) J Electroanal Chem 424:5
31. Uchida H, Hiei M, Watanabe M (1998) J Electroanal Chem 452:97
32. Santos MC, Miwa DW, Machado SAS (2000) Electrochem Commun 2:692
33. Llopis J F, Tordesillas IM (1978) In: Bard AJ (ed) Encyclopedia of electrochemistry of the elements, vol IV UMI. Marcel Dekker, New York
34. Hepel M (1999) In: Wieckowski A (ed) Interfacial electrochemistry, Chap 34. Marcel Dekker, New York, pp 599–630
35. Sauerbray G (1955) Z Phys 155:206
36. Juodkazis K, Stalnionios G, Sebeka B, Sukiene V, Savickaja I (2002) Russ J Electrochem 38:1157
37. Peuckert M (1984) Surface Sci 141:500